



# CARBONATE RESERVOIR CHARACTERIZATION USING THE CEMENTATION FACTOR: A CASE STUDY OF LITTLE CEDAR CREEK FIELD, ONSHORE ALABAMA

Qifei Huang and Yuefeng Sun

*Department of Geology and Geophysics, Texas A&M University, MS 3115, College Station, Texas 77843, U.S.A.*

## ABSTRACT

Facies characterization can be utilized to locate reservoir rocks. However, it alone cannot predict permeability and reservoir performance due to the complexity of pore type variation. In this paper, cementation factor “ $m$ ” in Archie's law is used to quantify the pore type variation in a microbial carbonate formation in onshore Alabama. From log and core analysis, we find that the dominant pores are: micropores ( $1 < m < 1.9$ ), intercrystalline and intergranular pores ( $1.9 < m < 2.1$ ), and vuggy pores ( $2.1 < m < 3$ ). The cementation factor deviation log is then introduced to assist in locating high permeability zones. The results show that the deviation in  $m$  agrees with the velocity deviation, both of which display a similar trend with permeability. Considering the similar impact of pore structure on resistivity and sonic velocity,  $m$  is further applied to estimate shear wave velocity and predict the amplitude versus offset (AVO) responses of reservoirs. The results show that rocks dominated by vuggy, moldic/intragranular, or microporosity display distinctive AVO features, and that fluid detection in carbonate rocks using conventional AVO classification is challenging.

## INTRODUCTION

Carbonate rocks generally have a low recovery factor due to a strong variation in pore type and permeability (Sheng, 2013). Changes in size, shape, and connectivity of the pores can significantly modify current and fluid flow. Many rock physics parameters have been proposed to characterize the pore structure variation (e.g. Anselmetti and Eberli, 1999; Sun, 2000). The cementation factor “ $m$ ” in Archie's equation has a strong dependence on the shape of grains and pores, and is so named the “shape factor” (Archie, 1942, 1952; Salem and Chilingarian, 1999). The value of  $m$  ranges from 1.8 to 4, which correlates with the percentage of vuggy porosity in total porosity (Lucia, 1983). Simple large pores such as vuggy, moldic pores have higher resistivity and cementation factor  $m$  while intricate small pores such as micropores have much lower resistivity and  $m$  (Verwer et al., 2011). Doveton (1999) reported that, in carbonate rocks, the value of  $m$  for intergranular or intercrystalline pore systems is 2, 1.4 for fractures, 2.4 for vuggy pores, and greater than 3 for moldic pores. Accordingly, the variation of permeability due to pore type change has been found to have a good relationship with cementation factor  $m$  from laboratory experiments. Samples with higher

permeability have higher cementation factors with a fixed porosity (Verwer et al., 2011).

Another challenging problem in carbonate rocks is that conventional amplitude versus offset (AVO) workflows for fluid detection may fail due to the pore structure effect (Sun, 2004). Sun (2004) found that AVO technology is better in fluid detection in carbonate rocks with only microporosity. For moldic rocks or rocks with a combination of micro-, inter-particle, and moldic porosities, it is difficult to distinguish water from hydrocarbons using AVO analysis. Instead, different pore types show different AVO characteristics. However, the modeling requires shear wave velocity data, which is often unavailable.

In this paper, the cementation factor  $m$  is first derived from resistivity and density logs acquired in the Smackover Formation, Little Cedar Creek Field, onshore Alabama. Then, an  $m$  deviation ( $\Delta m$ ) log is created by comparing  $m$  to a value of 2. Afterward,  $m$  and the  $m$  deviation ( $\Delta m$ ) log are investigated to characterize the pore type and permeability heterogeneity. The cementation factor  $m$  is further used as a pore structure indicator in a rock physics model to estimate shear wave velocity, considering the similar effect of pore structure on resistivity and velocity. The estimated shear velocity is integrated to model the AVO response of the studied carbonate reservoirs. Compared to the previous studies in the Smackover Formation of Little Cedar Creek Field focusing on depositional models and related facies (e.g., Mancini et al., 2006, 2008; Heydari and Baria, 2006; Ridgway, 2010), this study attempts to understand the petrophysical and seismic responses to the depositional variation. The applied

approach may be used to assist reservoir management in other fields producing from microbialites (e.g., Green River Formation and offshore Brazil).

## METHOD

### Pore Structure Index from Resistivity Log

We used the cementation factor  $m$  from Archie's equation (Archie, 1952) to quantify the pore type change and associated permeability behaviors in the Smackover Formation. The cementation factor  $m$  is calculated using the provided deep investigation resistivity ( $R_t$ ), apparent water saturation ( $R_{wa}$ ) logs and density derived porosity logs ( $\phi$ ), based on the following equations:

$$FF = \frac{R_t}{R_{wa}} \quad (1)$$

$$m = \frac{\log \frac{a}{FF}}{\log \phi} \quad (2)$$

where  $a$  is assumed to be 1, and  $FF$  is the formation factor. Density-derived porosity is calculated using a variable grain density based on the mineral compositions (Dou et al., 2011) and a constant fluid density of 1 g/cc. A constant fluid density is selected because there is very limited gas and oil show in the studied well from core observation. The derived porosity is further checked and corrected against core measurements where applicable. It is noted that the value of  $a$  is not always 1 and can vary between 0.5–1.5, following variations in lithology, pore structure and grain size (Winsauer et al., 1952). However, in carbonate rocks,  $a$  is close to 1. It is also noted that basic Archie's equation is chosen due to limited presence of clay in the studied interval.

Based on Equations 1 and 2, the cementation factor  $m$  is estimated at log scale. We then introduce a cementation factor deviation log ( $\Delta m$ ) by comparing the value of  $m$  to a value of 2. The concept of cementation factor deviation is similar to velocity deviation log introduced by Anselmetti and Eberli (1999), which is used as a tool for predicting of pore type and permeability. The deviation of velocity is made by comparing the sonic log velocity with the velocity calculated using the time-average equation of Wyllie (1956), as shown in Equation 3, which is valid for connected intergranular porosity. Similarly, the value of 2 is chosen to derive the cementation deviation log because it represents a rock frame with intergranular and intercrystalline pores (Dullien, 1992).

$$\frac{1}{V} = \frac{1-\phi}{V_m} + \frac{\phi}{V_f} \quad (3)$$

here the velocity of the matrix ( $V_m$ ) and water ( $V_f$ ) is taken to 6530 m/sec and 1500m/sec for this study, respectively. The values are chosen because the studied formation is mostly limestone and water wet. The cementation deviation log can be used to correlate the pore structure change to permeability in the same way the velocity deviation log can.

### Pore Structure Index Guided Shear Wave Estimation

In the studied field, a shear wave velocity log is not available and is estimated using Sun's (2000) rock physics model. Based on extended Biot theory (Biot, 1962a, 1962b), Sun (2000, 2004) introduced a rock physics model and defined elastic pa-

rameters, termed the frame flexibility factors ( $\gamma$ ,  $\gamma_\mu$ ), which are used as proxies for pore structure classification.

$$V_p = \sqrt{\frac{K + \frac{4}{3}\mu}{\rho}} \quad (4)$$

$$V_s = \sqrt{\frac{\mu}{\rho}} \quad (5)$$

$$K_d = K_s \cdot (1-\phi)^\gamma \quad (6)$$

$$\mu_d = \mu_s \cdot (1-\phi)^{\gamma_\mu} \quad (7)$$

For the studied reservoir rock, we assume that

$$K = K_d \quad (8)$$

$$\mu = \mu_d \quad (9)$$

where  $K$  and  $\mu$ ,  $K_d$  and  $\mu_d$ ,  $K_s$  and  $\mu_s$  are total, dry frame, solid matrix bulk modulus and shear modulus, respectively; and  $\gamma$  and  $\gamma_\mu$  are frame flexibility factors. Porosity ( $\phi$ ) is derived from density ( $\rho$ ).

Based on Equations 4–9, the shear wave velocity can be estimated as shown in Equation 10.

$$V_s = \frac{V_p}{\sqrt{(1-\phi)^{\gamma-\gamma_\mu} \frac{K_s}{\mu_s}}} \quad (10)$$

The derivation of  $V_s$  requires the input of a variable  $f$  (Equation 11) which is closely related to the pore structure.

$$f = (1-\phi)^{\gamma-\gamma_\mu} \quad (11)$$

When porosity or the pore connectivity increases, rocks become more susceptible to shear deformation than volumetric change (Detournay and Cheng, 1993). Both will result in a lowered  $f$  value. For instance, connected vuggy pores are much easier to deform than isolated moldic pores. As porosity and pore connectivity are the two most important factors deciding permeability behaviors, permeability can, in turn, infer the relative magnitude of  $f$ . We use the cementation factor  $m$  deviation ( $\Delta m$ ) log as a proxy for permeability, and thus estimate  $f$  as shown in Equation 12. The assumption is verified using the well log data from another field where  $V_s$  is available and will be discussed in the Results section.

$$\Delta m = cf \quad (12)$$

where  $f$  is a function of pore structure shown in Equation 11, and  $c$  is a constant for a specific rock type. The value of  $c$  will also be discussed in the Results section.

### Pore Structure AVO Modeling

With known  $V_p$ ,  $V_s$ , and  $\rho$ , AVO modeling is conducted at different angles using the AVO module available in Hampson-Russell Software (Russell, 2010), which is based on Zoeppritz equations (Zoeppritz, 1919). Three surfaces separating four major facies with distinctive pore types are selected to model the AVO response of seismic wave propagation. The effect of pore type on AVO response will be discussed in the Results section.

**FIELD DATA**

Little Cedar Creek Field (LCCF), onshore Alabama (Fig. 1), is an oil field with limited gas production. From 1994–2013, cumulative production is 20 million barrels of oil and condensate, and 19 million cubic ft of gas (Tonietto, 2014). The producing reservoirs are low-energy microbial thrombolite and oolitic grainstone of the Smackover Formation. The oolitic grainstone was deposited in a high-energy, near-shore environment on a carbonate ramp (Ahr, 1973) (Fig. 2). The ramp was created during sea level regression on the northeastern Gulf of Mexico platform, which was characterized as several marginal extensional basins created after the Early Triassic breakup of Pangea (Stanley, 2008). Following that, the Jurassic Smackover Formation was deposited within these basins. The deposition was compartmentalized by a series of structural highs (Heydari and Baria, 2006). Pre-Jurassic salt tectonics resulted in variations of topography (Ahr, 1973).

The post-rift deposition within the Gulf Coastal Plain is greatly affected by the Late Jurassic and Early Cretaceous transgression-regressive (T–R) sequences (Fig. 3). The Smackover Formation is deposited within one of the sequences, and is subdivided into the lower transgressive systems tract (TST) and upper highstand systems tract (HST). Five major facies formed following the sea level change. Transgressive lime-mudstone, microbial thrombolite, and microbially influenced packstone were deposited successively during the TST, following sea level rise. The maximum flooding zone is characterized by subtidal lime mudstone/wackestone and condensed section. Nearshore peloid/ooid grainstone and peritidal mudstone/dolostone have deposited afterward during HST when sea level drops (Mancini et al., 1990). Thrombolites with a clotted, mottled and nodular texture, and rare domal and branching structures, was deposited in nearshore, shallow subtidal paleoenvironments along the updip margin of Smackover Formation deposition (Mancini et al., 2008).

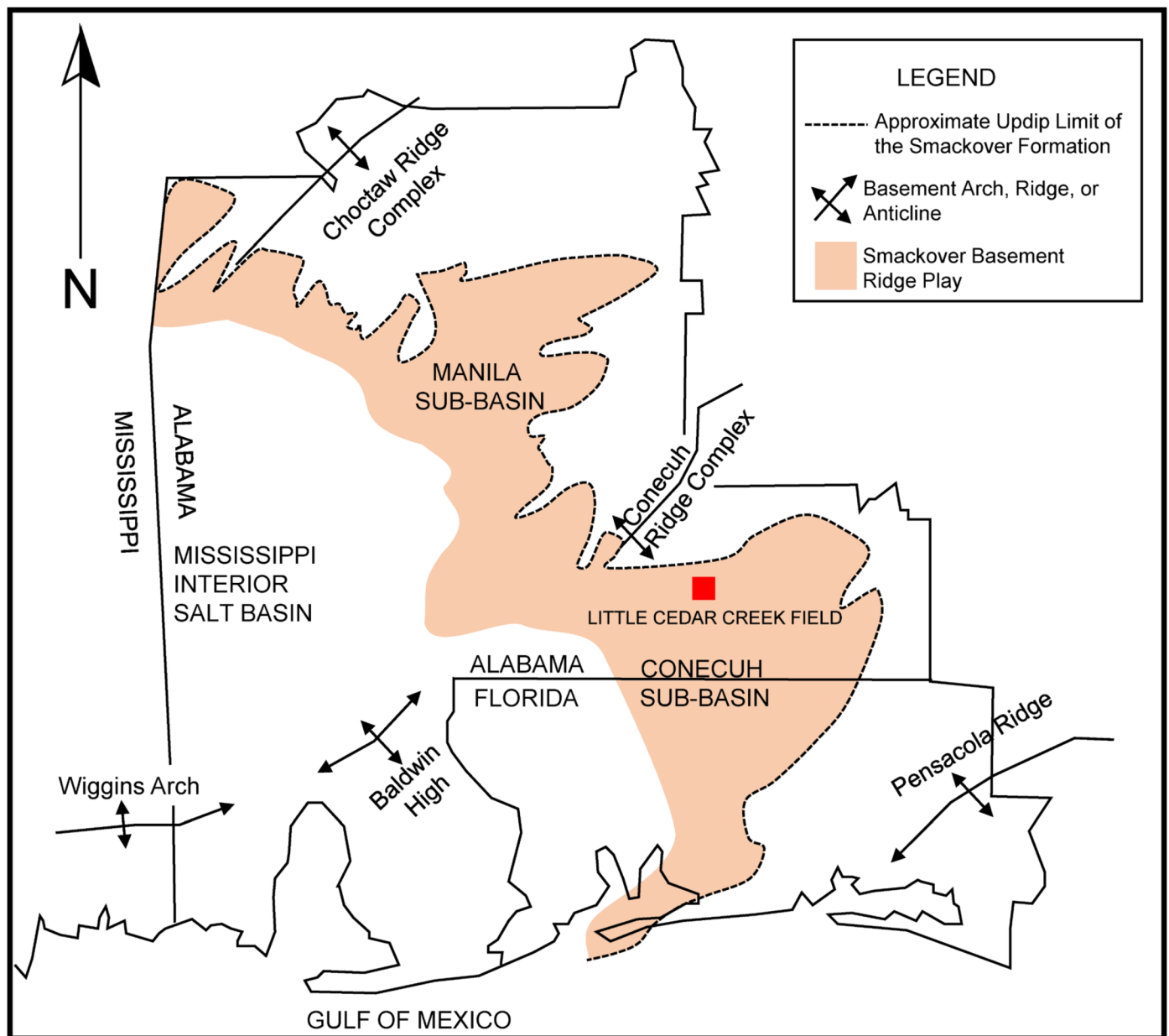


Figure 1. Regional structure map of the Gulf Coastal Plain, with information on the location of Little Cedar Creek Field and the distribution of the Smackover Formation (modified after Tonietto, 2014).

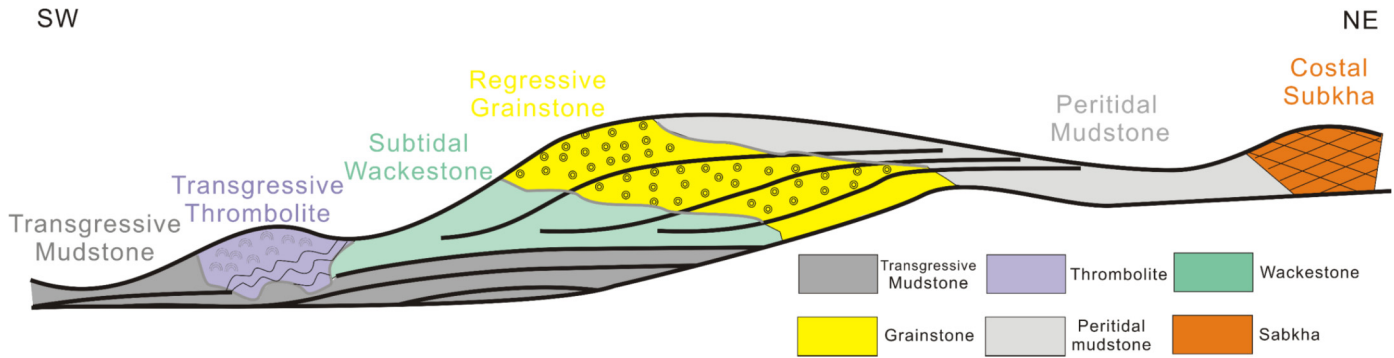


Figure 2. Depositional facies model for the Smackover Formation.

STAGE	T-R CYCLE	Formation	FACIES
OXFORDIAN	T	Haynesville (Buckner)	Anhydrite, Shale, and Sandstone
	SB		Peritidal Lime Mudstone/Dolostone
	R	Smackover	Peloid-Ooid Nearshore Higher Energy/Shoal Grainstone-Packstone
	smt		Subtidal Lime Wackestone-Lime Mudstone
	SSS		Microbially-Influenced Packstone-Wackestone
	T		Microbial (Thrombolite) Boundstone
	SB		Transgressive Lime Mudstone-Dolostone
	R	Morphlet	Conglomeratic Sandstone
T-Transgression R-Regression SB-Sequence Boundary smt-surface of maximum transgression sss-sediment starvation surface			

Figure 3. Sequence stratigraphy of Smackover Formation in Little Cedar Creek Field, Alabama (modified after Mancini et al., 2008).

The dominant pore types vary significantly as the facies change (Fig. 4). Vugs are mainly located in thrombolite facies developed during transgression. Microporosity is mostly found in transgressive mudstone and wackestone units at the end of transgression. Most of the grainstone unit consists of moldic pores generated by the dissolution of ooids after exposure during regression. Petrophysical properties vary significantly within the

thrombolite with porosity varying from 3 to 19% and permeability varying from less than 1 to 100 md, locally as much as 500 md (Tonietto, 2014). Dolomitization is limited and often occurs within the thrombolite facies in the southern portion of the field. The porosity for these intercrystalline pores varies between 10 to 21%, and permeability ranges from 150 to 850 md. Vugs developed from sucrosic intercrystalline pores create a much larger permeability that ranges from tens of md to hundreds of md. In comparison, most of the grainstone unit consists of moldic pores generated by the dissolution of ooids. The porosity is good, ranging from 5 to 32%. However, permeability within the grainstone unit is poor, varying from 1 to 10 md (Tonietto, 2014). Facies mapping assisted in the interpretation of pore types, characterizing pore structure, and finding reservoir zones. The limited amount of dolomitization and good preservation of depositional rock fabrics make it an excellent region to study the effects of depositional rock texture on petrophysical properties.

Conventional logging data from 81 wells were used in this work. Of the 81 wells, 27 wells have core data, and a few wells have special core analysis data. There is no shear log information available from the wells. Therefore, shear wave velocity will be estimated as outlined in the Methods section and then applied for seismic AVO modeling. The well used the most in this paper is from Well McCreary 21-1, which has 70 ft of core measurements such as porosity, permeability, thin sections, and core descriptions. Unfortunately, seismic reflection data (Handford and Baria, 2007) were not available for this study.

## RESULTS

### Pore Type Estimation

As shown in Figure 4, the Smackover Formation has diverse pore types for different facies units, which have significantly affected the rock properties. Figure 5 shows conventional logs and core measurements. Gamma ray (GR) and photoelectric factor (PEF) log shows that the studied interval is dominated by limestone matrix. The estimated matrix density and density porosity match well with the grain density and porosity from core lab measurement respectively, which the basis for an accurate estimation of  $m$ . Figure 5 also displays that grainstone and thrombolite have different resistivity values while both have lower porosity and velocity than mudstone. Thrombolite has higher average permeability than grainstone due to the occurrence of connected vuggy pores. Neither velocity nor porosity can distinguish the three facies noted alone. However, as illustrated in Figure 5, the calculated cementation factor  $m$  can be used to distinguish all three facies. The value of  $m$  for thrombolite is slightly larger than that for grainstone, while mudstone displays the smallest  $m$  among the three.

Figures 6 and 7 show the cross plots of  $FF$  and  $V_p$  against density porosity. For a given porosity, both  $FF$  and  $V_p$  show a

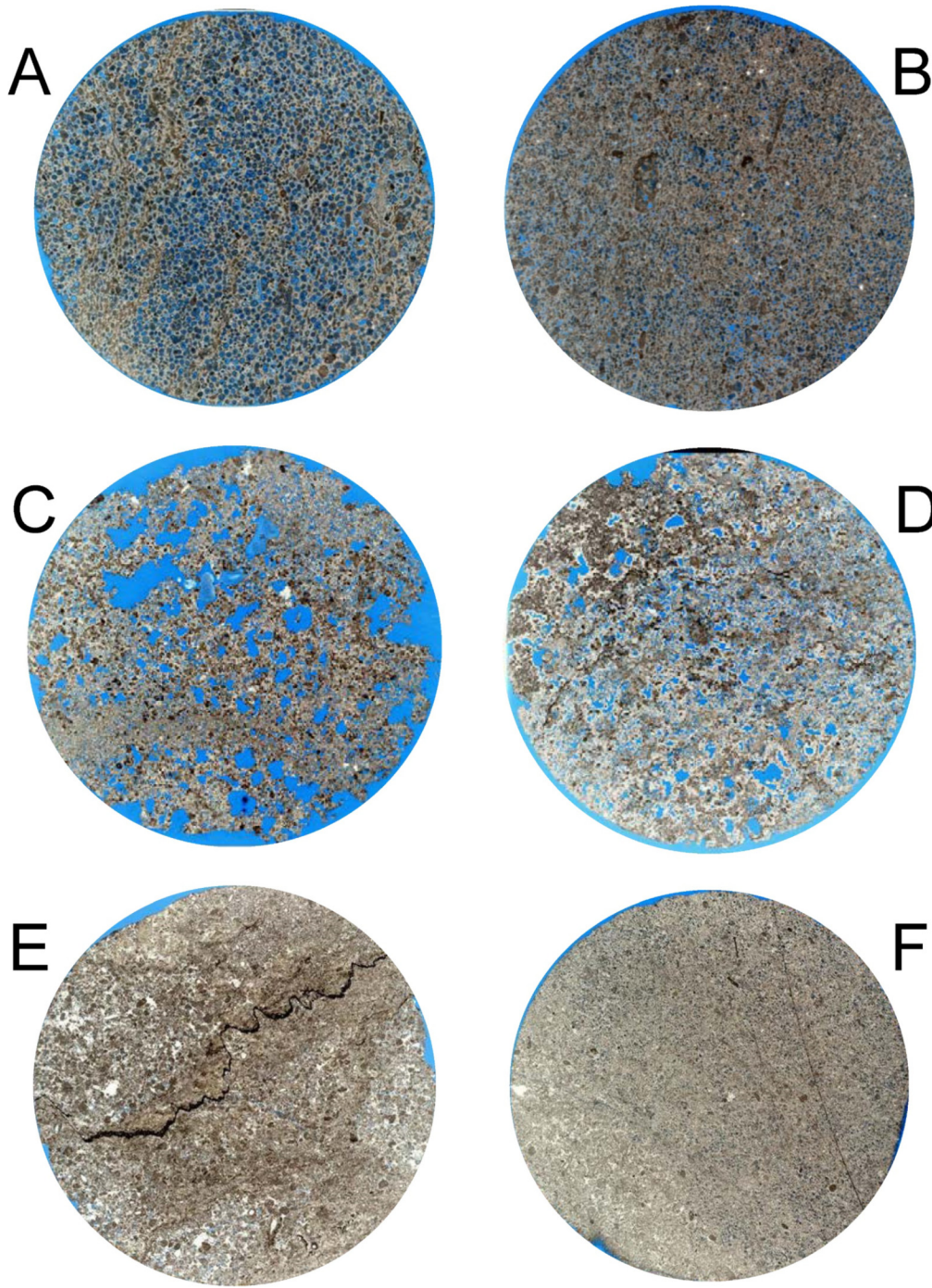


Figure 4. Images of scanned thin sections from 1 in (2.5 cm) diameter plugs, the blue color indicates pore spaces. The dominant features observed are (A, B) moldic porosity, (C) highly vuggy porosity, (D) intercrystalline and vuggy porosity, (E) stylolite and microporosity, and (F) highly cemented grainstone.

significant variation. Because the formation is relatively thin, in-situ pressure and temperature are considered to be constant, changes in pore structures cause the variations in  $FF$  and  $V_p$ . The cementation factor ( $m$ ) from Archie's law shows clear trends when used to study the scattered cross plots of formation factor and sonic velocity versus porosity due to its close relationship with reservoir pore structure. For  $m < 1.9$ ,  $FF$  and sonic velocity are low at a fixed porosity as microporosity dominates the rock. Micropores with larger pore numbers at a given porosity may result in better continuity for conducting electrical current and lower resistivity, while their relatively compliant rock mechanics lowers the velocity. Meanwhile, micropores restrict fluid flow with increased capillary actions, compared with larger pores at a given porosity. When  $1.9 < m < 2.1$ , the dominant pore type is interparticle or intercrystalline porosity. The interparticle pores in grainstone often occur with moldic porosity while intercrystal-

line porosity in thrombolite units are due to partial dolomitization. When  $2.1 < m < 3$ , the dominant pore type is vugs, widely distributed in thrombolites, which can be connected or isolated. Compared with microporosity at a given porosity, large vugs have a relatively low number of pores and create reduced flow paths for electrical charge resulting in higher resistivity. However, the permeability of these vugs for fluid can be high where vugs are connected with large pore throats as shown in Figure 4. For the very low porosity zone ( $< 2\%$ ), the  $FF$  and sonic velocity can be very high, and  $m$  can be larger than 3 because the rock is highly cemented and rigid.

### Permeability Evaluation

Carbonate pore type variation can significantly affect permeability by changing the pore throat size and connectivity. Ce-

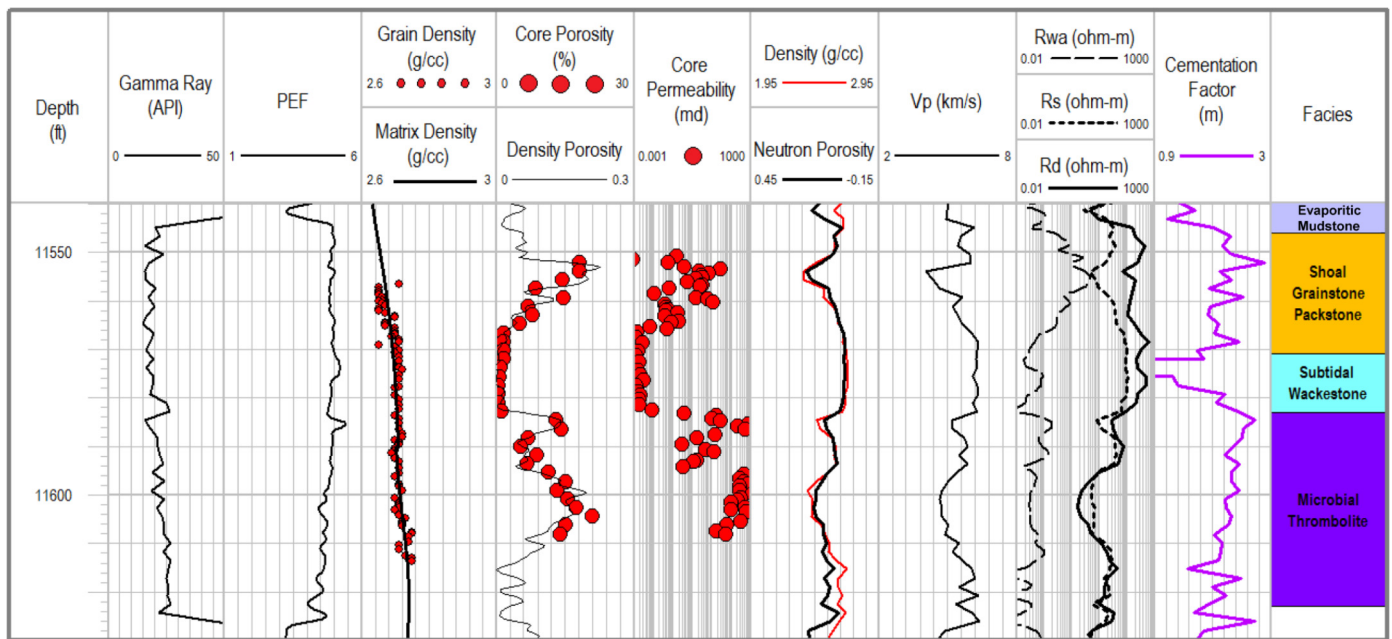


Figure 5. A representative conventional core and well log data for this study. The facies description and calculated cementation factor  $m$  are also illustrated.

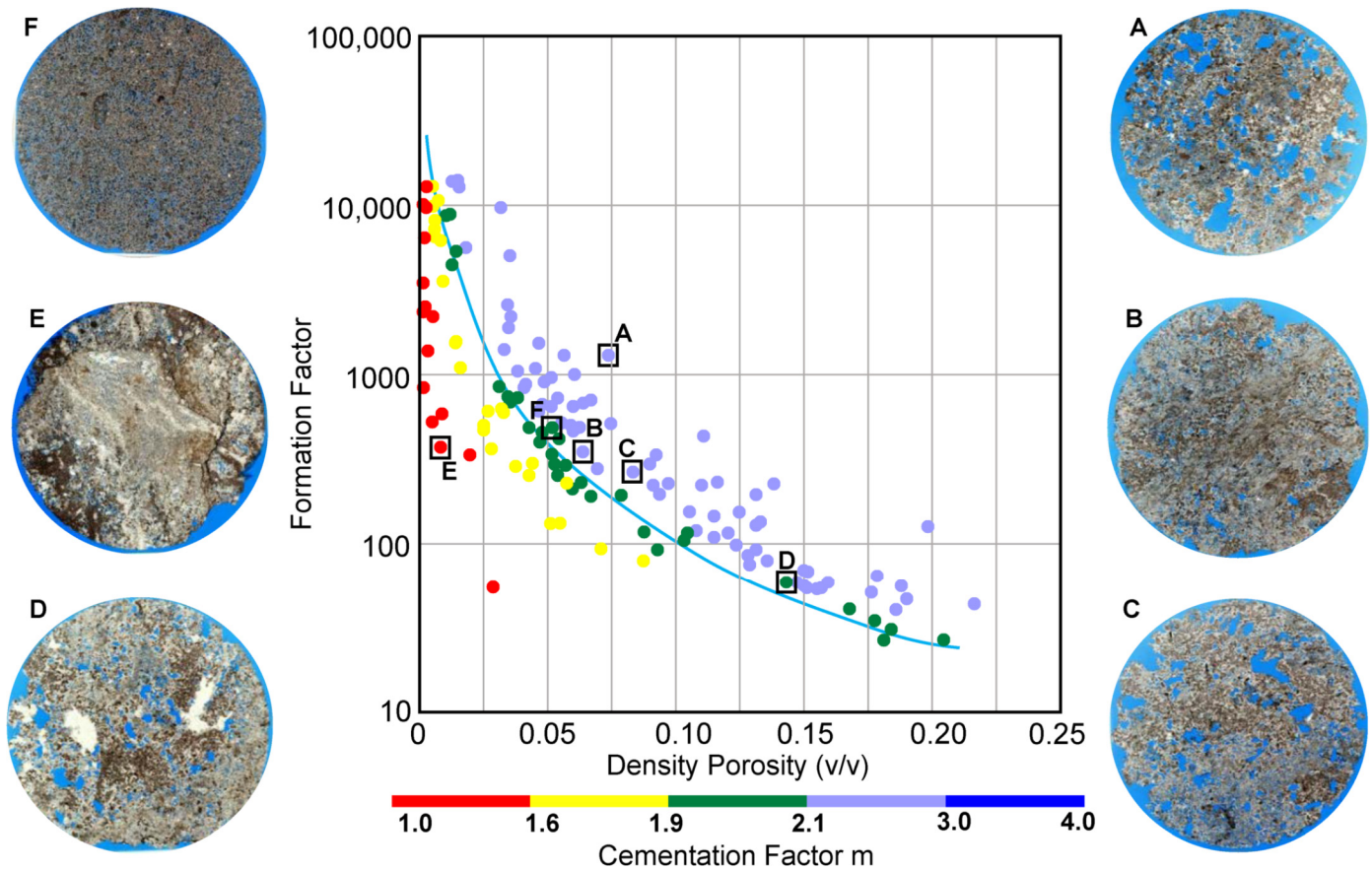


Figure 6. A plot of formation factor  $FF$  and corrected density porosity with cementation factor  $m$  being the color indicator. The green line shows the relation between  $FF$  and porosity when  $m$  is 2. Scanned thin sections from 1 in (2.5 cm) diameter plugs for the selected samples are also shown.

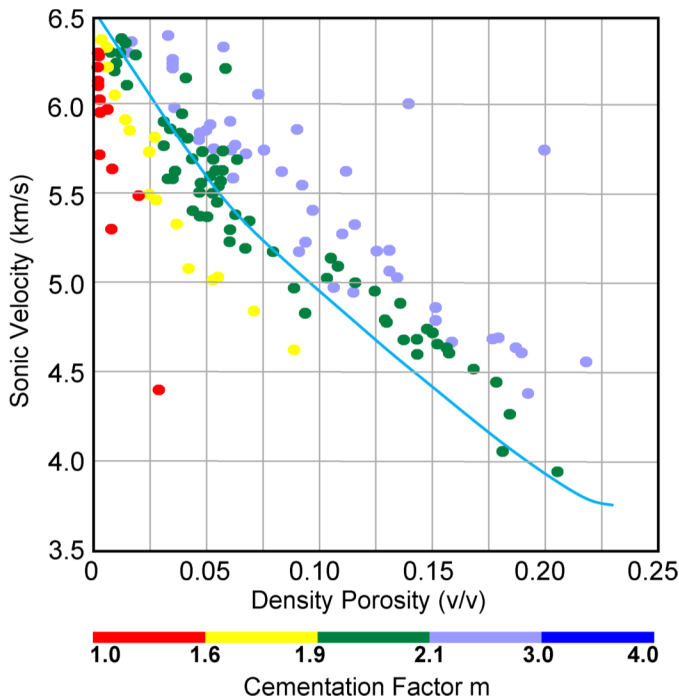


Figure 7. A plot of P-velocity and corrected density porosity with the cementation factor being the color indicator. The blue line shows the Wyllie's equation estimated velocity.

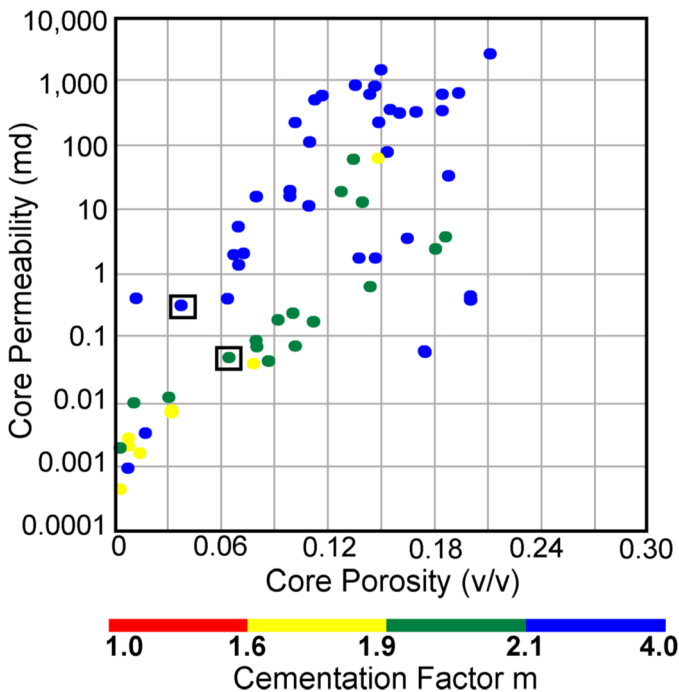


Figure 8. Semi-log plot of air permeability against porosity from core measurement. Cementation factor is the color indicator. Higher cementation factor displays higher permeability. The two blocks are data with thin sections shown in Figure 9.

mentation factor  $m$  as a pore structure indicator can be used to evaluate permeability. Figures 8 and 9 show that the moldic grainstone with a high cementation factor  $m$  has a relatively lower permeability. Thrombolites with a lower cementation factor

have higher permeability than moldic grainstone. Mudstone and wackestone with microporosity as the dominant pore type show the lowest cementation factor and lowest permeability. However, when fractures develop in the mudstone the permeability can increase. It is noted that although most of the rocks from the same facies have a similar range of value for  $m$ ,  $m$  can be quite variable within the same facies such as thrombolite.

In the Little Cedar Creek Field, the oolitic grainstone and thrombolite units are the two major reservoirs. However, the reservoir quality differs depending on the connectivity of moldic pores in grainstone and vugs in thrombolites. The thrombolite facies has a relatively large connected vuggy porosity, resulting in a higher  $m$  value and higher permeability than the grainstone unit. Therefore, the cementation factor deviation log can be used similarly to velocity deviation log to identify permeable zones (Fig. 10). The velocity deviation and cementation factor deviation are in agreement, both showing similar trends with permeability. This is especially true in high permeability zones which can be correlated with positive  $m$  and  $V_p$  deviation logs. The  $m$  deviation ( $\Delta m$ ) is as high as 0.9 with an average of 0.4 for the two zones. However, the deviation logs only provide a qualitative way to distinguish high permeable zones from less productive zones and cannot be applied to seismic. To understand the seismic responses of different pore types, AVO modeling is applied using the estimated shear wave velocity log.

### Shear Wave Estimation

In this study, the effect of cementation factor  $m$  on resistivity in Archie's law is mathematically similar to the influence of a predefined frame flexibility factors  $\gamma$  and  $\gamma_\mu$  on velocity in Sun's rock physics model, as shown in Equations 2 and 6 (Sun, 2004). The application of frame flexibility factors for pore type prediction is limited in this field due to insufficient shear wave velocity information. However, with given pore type information, this rock physics model can be used to estimate the shear wave velocity, which is needed to study the elastic properties of the rock and to create synthetic seismic models.

As outlined in Methods,  $m$  is used to classify the pore types and to obtain the solution to Equation 11 by searching for the  $c$  value in Equation 12. A well from Puguang Gas Field in Southwestern China, with shear velocity logs is first studied to test the assumed relationship between  $m$  and  $f$  in Equation 12. Puguang gas field is dominated in production from the Triassic Feixianguan Formation, which has similar pore types as occurred in Smackover Formation. The selected well has two distinctive pore types adjacently in the Triassic Feixianguan reservoir, namely intergranular and dissolution porosity (Ma et al., 2007; Yu et al., 2015). Figure 11 shows the cross plot of  $m$  against  $f$  based on the data from this well. The color indicates depth, where cooler colored samples are from interparticle pores, and warm colored samples are from dissolution pores. For the rock samples dominated by intergranular porosity,  $c$  is found to be around 0.5, while those dominated by dissolution porosity,  $c$  is around 2.5. Using the proposed methods, we estimated  $V_s$  for the reference well and compared the value to the  $V_s$  log, also shown in Figure 11. The estimated shear velocity agrees with the measured velocity.

Considering that the dominant pore types of Smackover Formation in LCCF are related to dissolution porosity,  $c$  is expected to be largely constant around 2.5 for this study. This is evident in the moldic porosity in upper oolitic grainstone unit and vuggy porosity in the lower thrombolite unit.

To further test this assumption, we apply different  $c$  values to the studied wells in LCCF and observe the correlations between core permeability and the calculated values of the two frame flexibility factors  $\gamma$  and  $\gamma_\mu$  (Fig. 12). Theoretically,  $\gamma$  and  $\gamma_\mu$  are good indicators of pore type (e.g. Dou, 2011; Adesokan and Sun, 2014; Zhang, 2014). The ratio of  $\gamma$  and  $\gamma_\mu$  is commonly

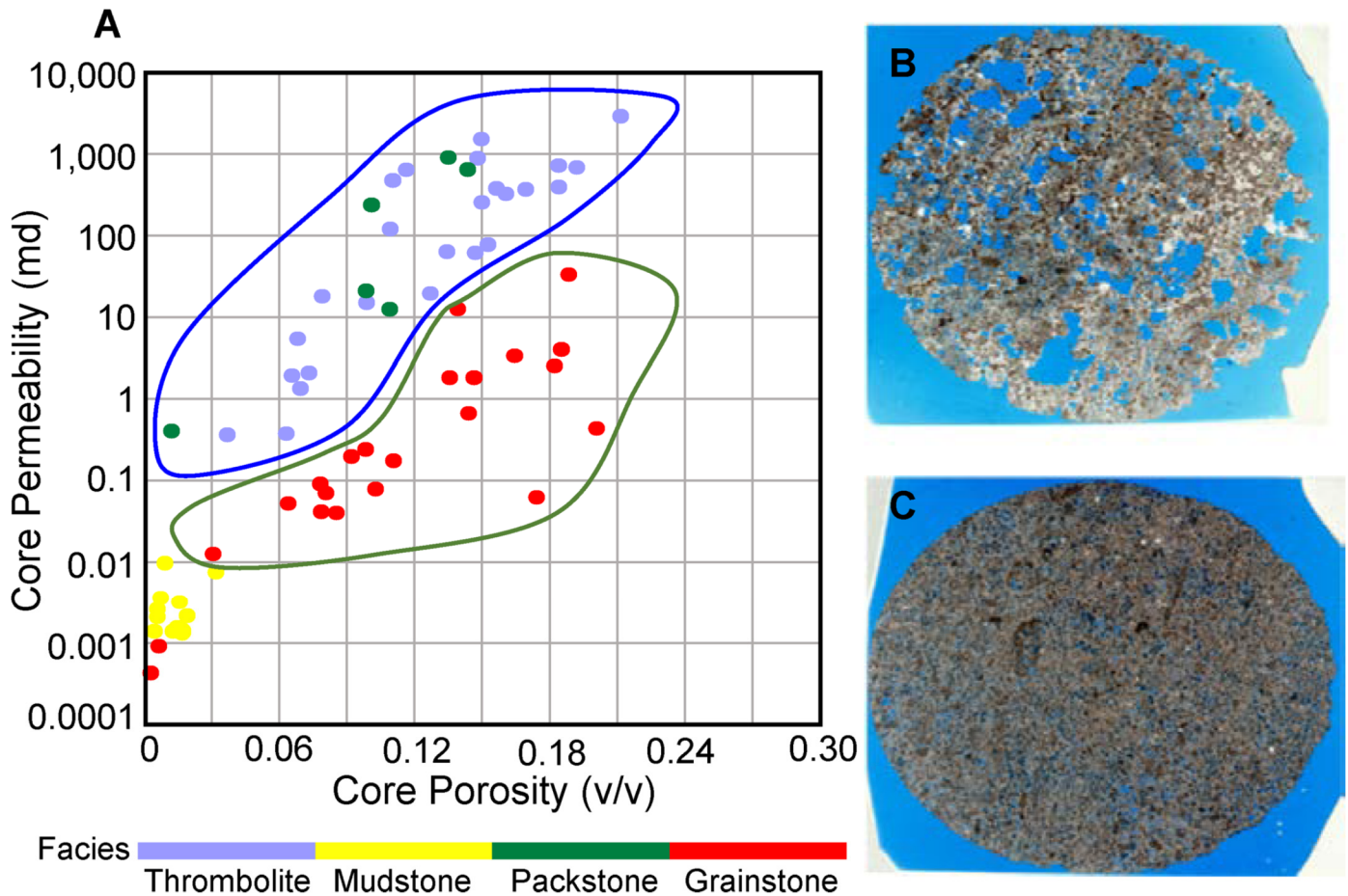


**Figure 9.** (A) Semi-log plot of air permeability against porosity from core measurements. The color is facies indicated with the purple dots representing microbial thrombolite, red representing ooidic grainstone, yellow representing mudstone. The most permeable zone for this well is in thrombolite unit. (B) Thin section of thrombolite at 11589.8 ft. (C) Thin section of the oolitic grainstone at 11561 ft.

considered as constant (Sun, 2004). The variation of both parameters should be similar and correlate with pore type variation. In this study, the permeability variation strongly agrees with the pore type variation, thus, the change of permeability should correspond to the variation of both factors. We assume that when the permeability variation agrees with  $\gamma$  and  $\gamma_\mu$  variations and the ratio of  $\gamma$  and  $\gamma_\mu$  is relatively stable, the estimated shear wave velocity is reliable. Based on this assumption, when  $c$  is 2.5,  $\gamma$  and  $\gamma_\mu$  best match the core permeability for the studied Smackover Formation. In addition, when  $c$  is 2.5, the variation of  $\gamma$  closely follows the variation of  $\gamma_\mu$  which makes the  $\gamma/\gamma_\mu$  ratio stable. We then can apply the estimated synthetic shear wave velocity from Equations 10–12 where  $c$  is 2.5, and then model the AVO responses of the studied reservoir.

### AVO Modeling

Seismic forward modeling is often necessary to assist with seismic interpretation and inversion. Amplitude versus offset (AVO) analysis has been widely used to predict fluid type. However, in carbonate rocks with complex rock texture, the AVO responses for the fluid are often disguised due to the strong influence of pore type on seismic wave propagation (Sun, 2004). The conventional AVO classification may not be applicable for carbonate reservoirs. Figure 13 shows the AVO responses of different pore types from Sun (2004) synthetic model. The two-layer model consists of a limestone reservoir of 30% porosity underlying a shale layer. The input parameters used for the model is also listed in Figure 13. The seismic signatures of three carbonate

pore types are modeled by solving Zoeppritz equation and applying elastic wave fine-element-method. AVO for fluid detection in oil saturated carbonate reservoirs is difficult due to the strong influence of pore structure on seismic wave propagation (Sun, 2004). However, the results show that there are distinctive features on AVO for different pore types.

Figure 14 shows the synthetic AVO modeling using the well log data ( $V_p$ ,  $V_s$ ,  $\rho$ ) from this study and a 30 Hz Ricker wavelet. We apply the backus average method to intervals above and below the three interfaces to get the average rock properties, which include the interfaces between overlying mudstone and grainstone, between grainstone and internal mudstone, between mudstone and thrombolite respectively. By solving the Zoeppritz equation using Hampson-Russell software, the synthetic signatures of the interfaces between different pore types are modeled (Russell, 2010). In agreement with Sun (2004), the synthetic seismic for the thrombolite unit, dominated by vuggy/intercrystalline pores, shows an abnormal amplitude increase near critical fraction followed by a sudden decrease in amplitude. The synthetic seismic for the grainstone unit, dominated by moldic/intergranular pores, shows a slight increase in amplitude near the critical angle followed by a sudden decrease in amplitude. The critical fraction angle in oolitic grainstone unit is around 12% larger than that the one in thrombolite. The synthetic seismic for mudstone with microporosity shows complete reversed polarity with no critical angle of refraction. These results can be used to direct and improve AVO prediction of pore structure and high permeability zones when pre-stack data is available.

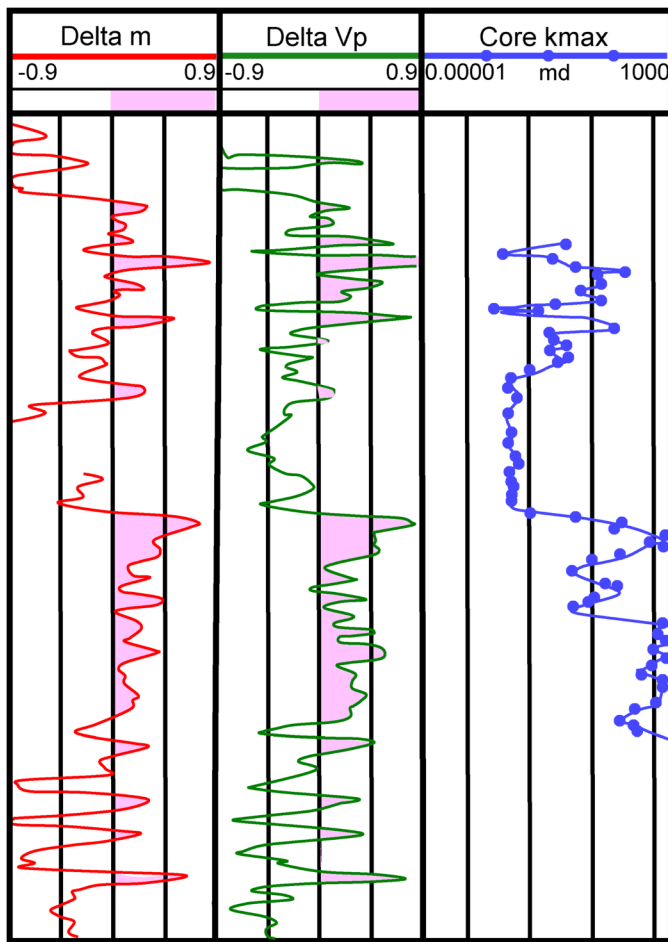


**Figure 10.** Log template showing cementation factor deviation curve, velocity deviation curve, and permeability curve. The predicted high permeability zone is indicated by pink color.

## CONCLUSIONS

In this study, the cementation factor “ $m$ ” and its deviation log are found to effectively describe the pore structure variation and permeability heterogeneity in a microbial carbonate formation onshore Alabama. When  $1 < m < 1.9$ , the dominant pore type is micropores; when  $1.9 < m < 2.1$ , the dominant pore types are intercrystalline and intergranular; when  $2.1 < m < 3$ , vuggy pores are prevalent. The deviation of  $m$  correlates with the permeability variation. The cementation factor  $m$  is then applied in a rock physics model to estimate shear wave velocity and model the AVO responses of pore structures. The 1D synthetic seismic modeling for the lower thrombolite and upper grainstone units show similar increasing amplitude with offset followed by a sudden decrease in amplitude near the critical fraction. When compared to thrombolite, the offset for the critical fraction in grainstone is 12% larger. In contrast, mudstone with microporosity shows a slight decrease followed by a sudden increase in amplitude near the critical fraction. The offset for the critical fraction in mudstone is the largest among the three rock types. These results can be used to direct AVO prediction of pore type and permeability in microbial carbonate reservoirs when pre-stack data are available.

## ACKNOWLEDGMENTS

The authors are grateful to the Department of Geology and Geophysics, Texas A&M University for its financial support.

We thank Dr. Ernest Mancini and Dr. Michael Pope for the dataset.

## REFERENCES CITED

- Adesokan, H., and Y. F. Sun, 2014, Rock-physics-based estimation of critical-clay-volume fraction and its effect on seismic velocity and petrophysical properties: *Geophysics*, v. 79, p. D175–D185, doi:10.1190/geo2012-0510.1.
- Ahr, W. M., 1973, The carbonate ramp: An alternative to the shelf model: *Gulf Coast Association of Geological Societies Transactions*, v. 23, p. 221–225.
- Anselmetti, F. S., and G. P. Eberli, 1999, The velocity-deviation log: A tool to predict pore type and permeability trends in carbonate drill holes from sonic and porosity or density logs: *American Association of Petroleum Geologists Bulletin*, v. 83, p. 450–466.
- Archie, G. E., 1942, The electrical resistivity log as an aid in determining some reservoir characteristics: *Transactions of the American Institute of Mining and Metallurgical Engineers*, v. 146, p. 54–61, doi:10.2118/942054-G.
- Archie, G. E., 1952, Classification of carbonate reservoir rocks and petrophysical considerations: *American Association of Petroleum Geologists Bulletin*, v. 36, p. 278–298.
- Biot, M. A., 1962a, Generalized theory of acoustic propagation in porous dissipative media: *The Journal of the Acoustical Society of America*, v. 34, p. 1254–1264, doi:10.1121/1.1918315.
- Biot, M. A., 1962b, Mechanics of deformation and acoustic propagation in porous media: *Journal of Applied Physics*, v. 33, p. 1482–1498, doi:10.1063/1.1728759.
- Detournay, E., and A. H. D. Cheng, 1993, Fundamentals of poroelasticity, analysis and design methods, in J. A. Hudson, ed., *Comprehensive rock engineering*, v. 2: Pergamon Press, Oxford, U.K., p. 113–171.
- Dou, Q. F., 2011, Rock physics-based carbonate reservoir pore type evaluation by combining geological, petrophysical and seismic data: Ph.D. Dissertation, Texas A&M University, College Station, 157 p., <<http://hdl.handle.net/1969.1/ETD-TAMU-2011-05-9502>> Last accessed September 20, 2017.
- Dou, Q. F., Y. F. Sun, and C. Sullivan, 2011, Rock-physics-based carbonate pore type characterization and reservoir permeability heterogeneity evaluation, Upper San Andres reservoir, Permian Basin, West Texas: *Journal of Applied Geophysics*, v. 74, p. 8–18, doi:10.1016/j.jappgeo.2011.02.010.
- Doveton, J. H., 1999, Basics of oil and gas log analysis: *Kansas Geological Survey, Lawrence*, 36 p., <<http://www.kgs.ku.edu/PRS/Info/pdf/doveton.PDF>> Last accessed September 20, 2017.
- Dullien, F. A. L., 1992, Porous media-fluid transport and pore structure: Academic Press, San Diego, California, 574 p., doi:10.1002/aic.690380819.
- Handford, C. R., and L. R. Baria, 2007, Geometry and seismic geomorphology of carbonate shoreface clinoforms, Jurassic Smackover Formation, North Louisiana: *Geological Society of London Special Publications*, v. 277, U.K., p. 171–185, doi:10.1144/GSL.SP.2007.277.01.10.
- Heydari, E., and L. R. Baria, 2006, Reservoir characteristics of the Smackover Formation at the Little Cedar Creek Field, Conecuh County, Alabama: *Gulf Coast Association of Geological Societies Transactions*, v. 56, p. 283–289.
- Lucia, F. J., 1983, Petrophysical parameters estimated from visual descriptions of carbonate rocks: A field classification of carbonate pore space: *Journal of Petroleum Technology*, v. 35, p. 629–637, doi:10.2118/10073-PA.
- Ma, Y. S., X. S. Guo, T. L. Guo, R. Huan, X. Y. Cai, and G. X. Li, 2007, The Puguang Gas Field: New giant discovery in the Mature Sichuan Basin, southwest China: *American Association of Petroleum Geologists Bulletin*, v. 91, p. 627–643, doi:10.1306/11030606062.
- Mancini, E. A., W. C. Parcell, and W. M. Ahr, 2006, Upper Jurassic Smackover thrombolite buildups and associated nearshore facies, southwest Alabama: *Gulf Coast Association of Geological Societies Transactions*, v. 56, p. 551–563.

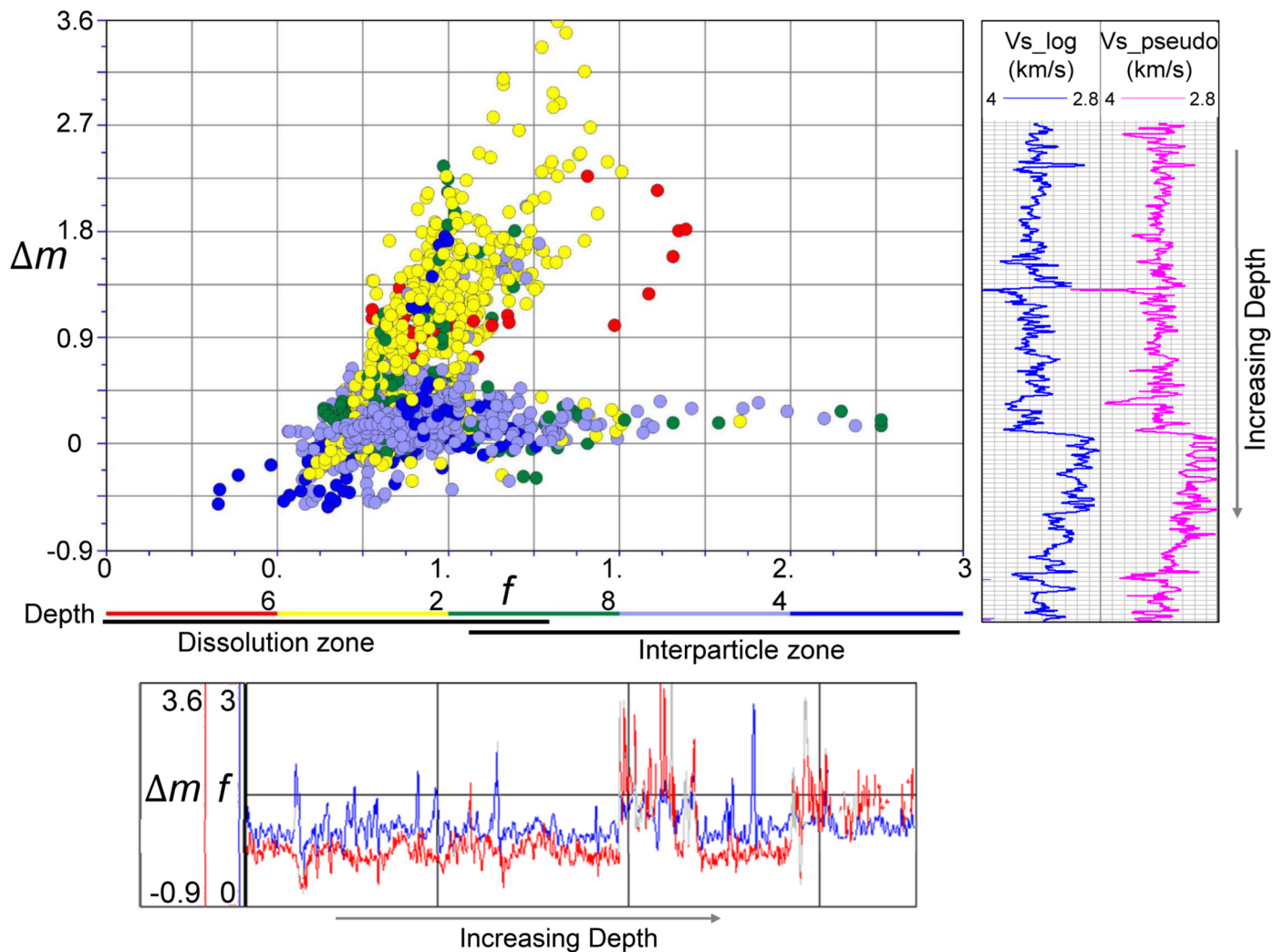


**Figure 11.** Cross-plot of cementation factor  $m$  against the calculated  $f$  factor from Equation 11 using the well log data from another field. The calculated log curves for  $m$  and  $f$  factor are also displayed for the studied interval.

- Mancini, E. A., W. C. Parcell, W. M. Ahr, V. O. Ramirez, J. C. Llinas, and M. Cameron, 2008, Upper Jurassic updip stratigraphic trap and associated Smackover microbial and nearshore carbonate facies, eastern Gulf Coastal Plain: *American Association of Petroleum Geologists Bulletin*, v. 92, p. 417–442, doi:10.1306/11140707076.
- Mancini, E. A., B. H. Tew, and R. M. Mink, 1990, Jurassic sequence stratigraphy in the Mississippi Interior Salt Basin of Alabama: *Gulf Coast Association of Geological Societies Transactions*, v. 40, p. 521–529.
- Ridgway, J. G., 2010, Upper Jurassic (Oxfordian) Smackover facies characterization at Little Cedar Creek Field, Conecuh County, Alabama: M.S. Thesis, University of Alabama, Tuscaloosa, 128 p.
- Russell, B., 2010, Making sense of all that AVO and inversion stuff: The Milton Dobrin lecture, <<http://www.agl.uh.edu/pdf/russell-2010.pdf>> Last accessed September 20, 2017.
- Salem, H. S., and G. V. Chilingarian, 1999, The cementation factor of Archie's equation for shaly sandstone reservoirs: *Journal of Petroleum Science and Engineering*, v. 23, p. 83–93, doi:10.1016/S0920-4105(99)00009-1.
- Sheng, J., ed., 2013, *Enhanced oil recovery field case studies*: Gulf Professional Publishing, Waltham, Massachusetts, 712 p.
- Stanley, S. M., 2008, *Earth system history*, 3rd ed.: W. H. Freeman, New York, New York, 615.
- Sun, Y. F., 2000, Core-log-seismic integration in hemipelagic marine sediments on the eastern flank of the Juan de Fuca Ridge: *Proceedings of the Ocean Drilling Program. Scientific results*, p. 21–35, doi:10.2973/odp.proc.sr.168.009.2000.
- Sun, Y. F., 2004, Pore structure effects on elastic wave propagation in rocks: AVO modelling: *Journal of Geophysics and Engineering*, v. 1, p. 268–276, doi:10.1088/1742-2132/1/4/005.
- Tonietto, S., 2014, Pore characterization and classification in carbonate reservoirs and the influence of diagenesis on the pore system. Case Study: Thrombolite and grainstone units of the Upper Jurassic Smackover Formation, Gulf of Mexico: Ph.D. Dissertation, Texas A&M University, College Station, 578 p., <<http://hdl.handle.net/1969.1/154204>> Last accessed September 20, 2017.
- Verwer, K., G. P. Eberli, and R. J. Weger, 2011, Effect of pore structure on electrical resistivity in carbonates: *American Association of Petroleum Geologists Bulletin*, v. 95, p. 175–190, doi:10.1306/06301010047.
- Winsauer, W. O., H. M., Shearin, Jr., P. H., Masson, and M. Williams, 1952, Resistivity of brine-saturated sands in relation to pore geometry: *American Association of Petroleum Geologists Bulletin*, v. 362, p. 253–277.
- Wyllie, M. R. J., A. R. Gregory, and L. W. Gardner, 1956, Elastic wave velocities in heterogeneous and porous media: *Geophysics*, v. 21, p. 41–70, doi:10.1190/1.1438217.
- Yu, Y., X. C. Tan, P. Y. Chen, H. T. Yang, T. Ma, J. Cao, and X. J. Jin, 2015, Discovery of hiatus in Feixianguan Formation and its geological implications, Sichuan Basin, SW China:

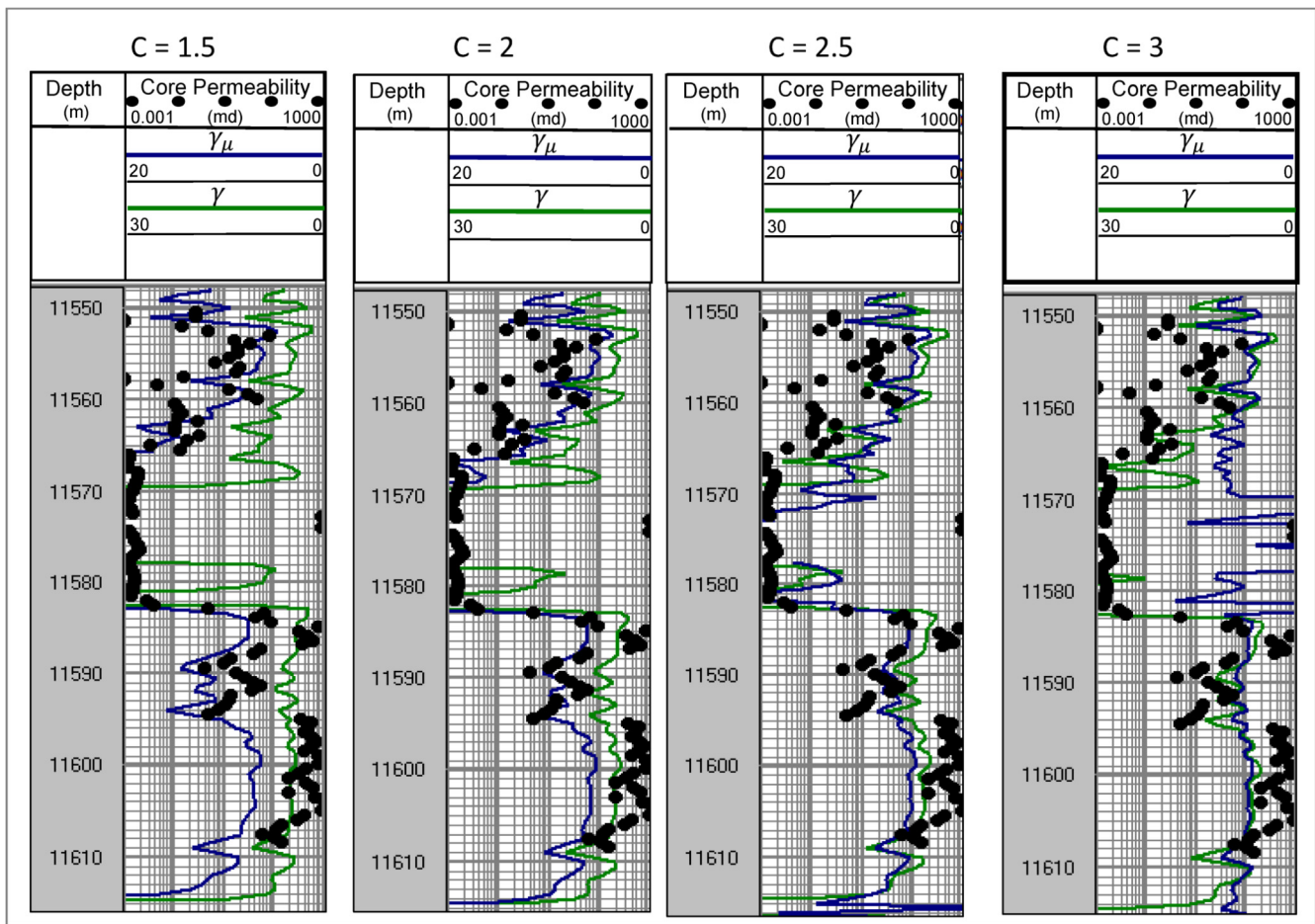
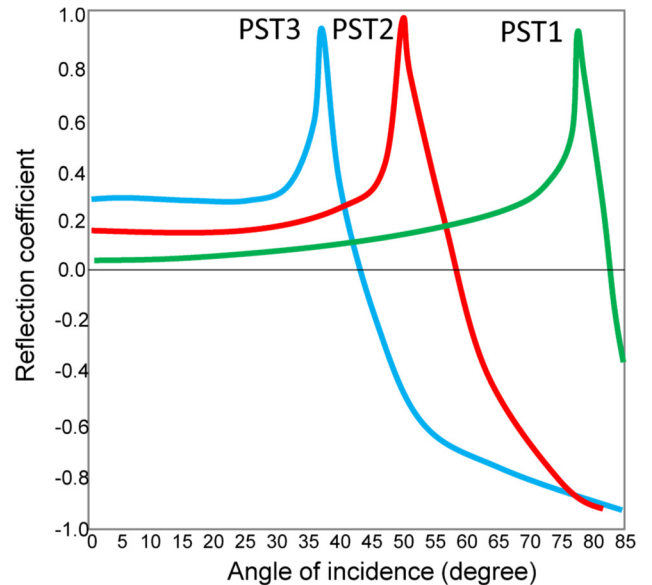


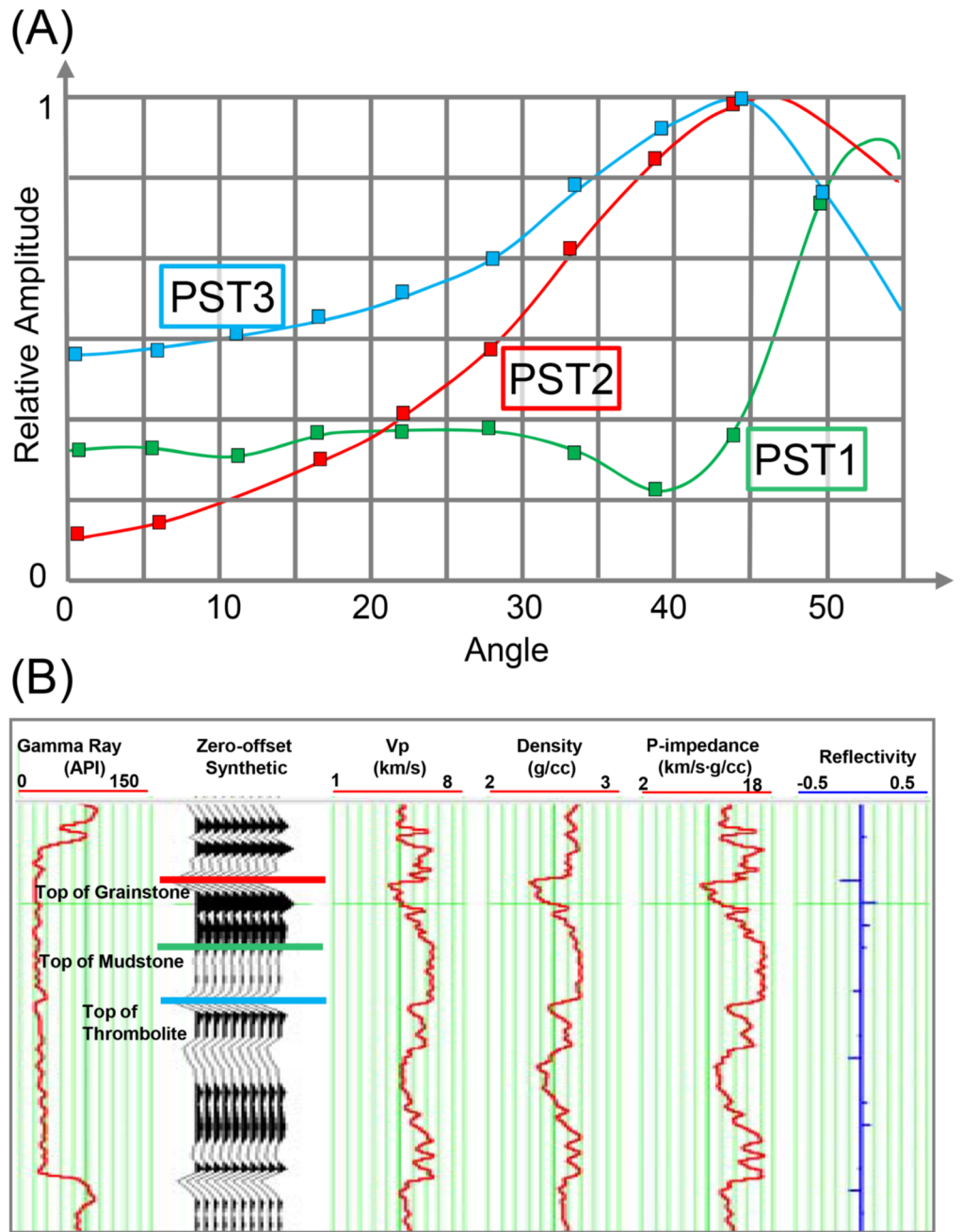
Figure 12. Comparison of core permeability with the calculated frame flexibility factors based on different  $c$  values.

Figure 13. Synthetic modeling of P-wave reflection for a shale/limestone interface for water saturated rocks dominated by three different pore types (modified after Sun, 2004). PST1 is dominated by microporosity, PST2 represents moldic rocks with or without vugs, PST3 is from a mixture of interparticle and vuggy porosity.



Rock Type	PST	Density (g/cc)	Vp (km/s)	Vs (km/s)
Shale		2.06	2.73	1.39
Limestone	1	2.13	2.81	1.14
Limestone	2	2.13	3.61	1.67
Limestone	3	2.13	4.61	2.26

Figure 14. (A) Synthetic modeling of P-wave reflection for the top of grainstone unit (red), top of mudstone unit (green), and top of thrombolite unit (blue), respectively. The grainstone and thrombolite are reservoirs while mudstone is non-reservoir. (B) The synthetic zero-offset seismic trace and its corresponding elastic properties for the studied well.



Turkish Journal of Earth Sciences, v. 24, p. 39–55, doi:10.3906/yer-1410-7.

Zhang, T. T., 2014, Integration of rock physics and seismic inversion for carbonate reservoir characterization, dissertation, Texas A&M University, College Station, <http://

hdl.handle.net/1969.1/154204> Last accessed September 20, 2017.

Zoeppritz, K., 1919, On the reflection and propagation of seismic waves at discontinuities: *Erdbebenwellen*, v. 7B, p. 66–84.